

AD A121946

NOSC TR 716

# NOSC

NOSC TR 716

Technical Report 716

## TEMPERATURE EFFECTS IN CERAMIC RESONATORS CONTAINING CEMENT JOINTS

C.L. Goodhart  
G.L. Kinnison  
C.I. Bohman  
G.W. Benthien

June 1982

Interim Report: October 1980–September 1981

Prepared for:  
Naval Research Laboratory/Underwater  
Sound Reference Detachment (NR/USRD)  
Orlando FL 32856

Approved for public release; distribution unlimited

NAVAL OCEAN SYSTEMS CENTER  
SAN DIEGO, CALIFORNIA 92152

82 12 01 009

DEC 1 1982

A

DTIC FILE COPY



NAVAL OCEAN SYSTEMS CENTER, SAN DIEGO, CA 92152

**AN ACTIVITY OF THE NAVAL MATERIAL COMMAND**

**JM PATTON, CAPT. USN**  
Commander

**HL BLOOD**  
Technical Director

**ADMINISTRATIVE INFORMATION**

The work reported herein was performed under Sensors and Spatial Processing Division (Code 712) for the U.S. Navy. The work was supported by the Naval Research Laboratory/Underwater Sound Reference Detachment from October 1980 through September 1981 under NOSC 712-WS55-S0219AS, program element 64503N. The work follows an initial effort supported by Naval Sea Systems Command in FY 1980.

Released by  
D. L. Carson, Head  
Sensors and Spatial  
Processing Division

Under authority of  
H. A. Schenk, Head  
Undersea Surveillance  
Department

**ACKNOWLEDGEMENTS**

The authors thank H.H. Ding for his valuable assistance with the experimental instrumentation and resonator computer modeling efforts as well as his participation in many fruitful discussions concerning this study. We are also grateful to J.J. Cross for his assistance in obtaining much of the experimental data, to L.E. McCleary for his role in obtaining the resonator modeling results, to C. Clark (NAVSEA) for sponsoring the initial investigation into this problem in FY80, and to R.W. Timme (NRL) for sponsoring the work presented here.



1. Title		<input checked="" type="checkbox"/>
2. Author		<input type="checkbox"/>
3. Subject		<input type="checkbox"/>
4. Distribution		
5. Distribution/Availability Codes		
6. Avail and/or Special		
A		

**CONVERSION TO METRIC**

1.0 inch  $\approx$  2.5 cm  
1.0 lb  $\approx$  0.45 kg  
0°F  $\approx$  -17.8°C

UNCLASSIFIED

SECURITY CLASSIFICATION OF THIS PAGE (When Data Entered)

REPORT DOCUMENTATION PAGE		READ INSTRUCTIONS BEFORE COMPLETING FORM
1. REPORT NUMBER NOSC Technical Report 716 (TR 716)	2. GOVT ACCESSION NO. AD-A121940	3. RECIPIENT'S CATALOG NUMBER
4. TITLE (and Subtitle) TEMPERATURE EFFECTS IN CERAMIC RESONATORS CONTAINING CEMENT JOINTS		5. TYPE OF REPORT & PERIOD COVERED Interim report, October 1980 - September 1981
		6. PERFORMING ORG. REPORT NUMBER
7. AUTHOR(s) CL Goodhart                      CI Bohman GL Kinnison                      GW Benthien		8. CONTRACT OR GRANT NUMBER(s)
9. PERFORMING ORGANIZATION NAME AND ADDRESS Naval Ocean Systems Center San Diego, California 92152		10. PROGRAM ELEMENT, PROJECT, TASK AREA & WORK UNIT NUMBERS 712-WS55, S0219AS, 64503N
11. CONTROLLING OFFICE NAME AND ADDRESS Naval Research Laboratory, Orlando FL		12. REPORT DATE June 1982
		13. NUMBER OF PAGES 28
14. MONITORING AGENCY NAME & ADDRESS (if different from Controlling Office)		15. SECURITY CLASS. (of this report) Unclassified
		15a. DECLASSIFICATION/DOWNGRADING SCHEDULE
16. DISTRIBUTION STATEMENT (of this Report)  Approved for public release; distribution unlimited		
17. DISTRIBUTION STATEMENT (of the abstract entered in Block 20, if different from Report)		
18. SUPPLEMENTARY NOTES		
19. KEY WORDS (Continue on reverse side if necessary and identify by block number) ceramic stacks cement joints piezoelectric ceramic sonar transducers		
20. ABSTRACT (Continue on reverse side if necessary and identify by block number) A temperature-related performance degradation has been discovered in ceramic stack 33-mode resonators that employ cement joints. This study sought to identify the mechanism that has produced this performance degradation and to determine resonator design improvements that eliminate or limit this degradation. A computer model of a typical ceramic stack resonator has been modified to include cement joints and has been used to simulate resonator in-air performance as a function of ceramic and cement-joint parameters. Experimental tests and initial modeling results indicate that temperature effects in the cement joints are the chief source of the resonator temperature-related performance degradation. The performance improvement that results from increased stress bias on the resonator during cement curing appears to be due to reduced amounts of cement in the joints.		

DD FORM 1473

1 JAN 73

EDITION OF 1 NOV 68 IS OBSOLETE

S/N 0102-LF-014-6601

UNCLASSIFIED

SECURITY CLASSIFICATION OF THIS PAGE (When Data Entered)

## SUMMARY

### PROBLEM

In November of 1978, a number of prototype sonar transducers were observed to exhibit current runaway when driven continuously by a high-level constant-voltage source. Experimental tests indicated the source of the problem to be temperature-related performance degradation of the ceramic stack resonators used in the transducers.

### OBJECTIVE

Identify the mechanism that has produced temperature-related performance degradation of ceramic stack resonators. Determine design improvements to eliminate or limit the degrading temperature effects.

### RESULTS

A computer model of a typical ceramic stack resonator has been modified to include cement joints and has been used to simulate resonator in-air performance as a function of ceramic and cement-joint parameters.

Experimental tests and initial modeling results indicate that temperature effects in the cement joints are the chief source of the resonator performance degradation at high temperatures.

The improvement in the temperature-related resonator performance that results from increased stress bias on the resonator during cement curing appears to be due to reduced amounts of cement in the joints.

### RECOMMENDATIONS

Further work is necessary to extend the modeling results to include temperature dependence and radiation loading on the resonator (so far, model

simulations have only been for a resonator in air). The following is a list of recommended tasks:

1. Obtain ceramic and cement-joint parameter vs temperature data.
2. Apply the proper temperature-dependent ceramic and cement joint parameters to in-air and radiation-loaded resonator models (perhaps guided by surface temperature measurements of in-air and dummy-loaded resonators) in order to obtain resonator performance as a function of temperature.
3. Exercise this "temperature-dependent" model in order to draw conclusions about the role of cement joints in the ceramic stack resonator temperature-dependent performance and determine general methods to eliminate or limit the cement-joint effects.

## CONTENTS

Background . . .	Page 4
Experimental Evidence of Cement-Joint Problems . . .	8
Resonator Computer Model . . .	16
Modeling Results . . .	21
Conclusions . . .	27
Recommendations . . .	27
References . . .	28

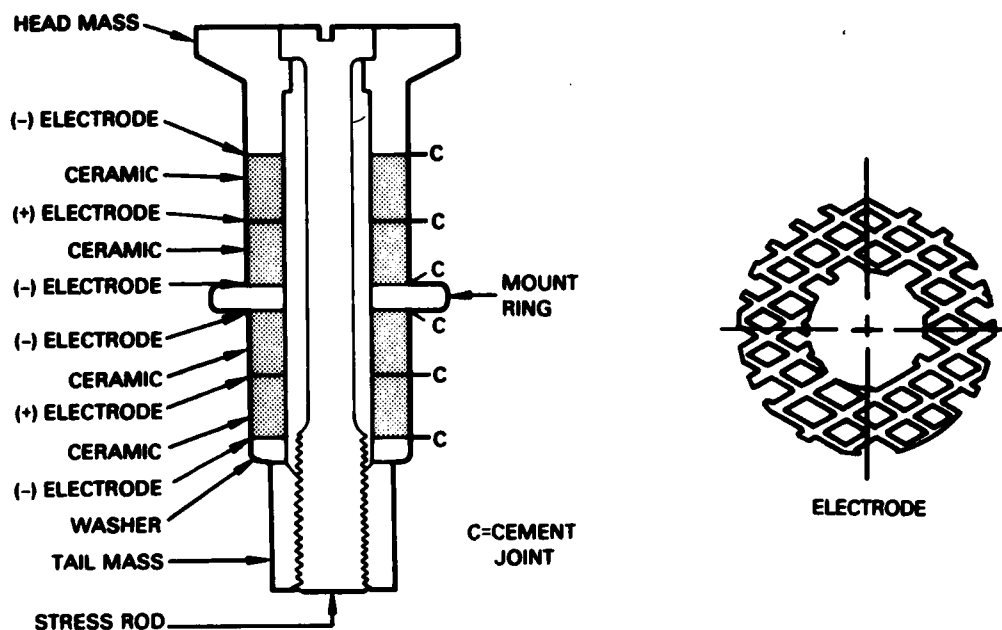
## BACKGROUND

In November of 1978, prototype sonar transducers were tested at constant-voltage, high drive levels during composite-unit accelerated life testing (CUALT). In most of the units tested, the electrical input impedance was observed to decrease with drive time (although initially a slight increase usually occurred), resulting in a current-runaway situation. The current rise was also noted to be accompanied by a temperature rise in the transducer. The current-runaway situation when left unchecked would eventually cause the transducer to fail because of excessive heating. In units where the current was not allowed to rise high enough to cause failure, the transducer recovered after cooling and showed no signs of permanent deterioration. Transducers placed in a water barrel, with the tuning section not immersed, showed a lowering of electrical input impedance with increases of water temperature. This focused attention on the transducers and not the tuning elements in seeking the cause for the current runaway and, in addition, showed that the problem was temperature related.

The transducers consist of staves of ceramic-stack longitudinal (33-mode) resonators of the type shown in Figure 1. The resonators employ piezoelectric ceramic rings that are cemented together in order to ensure good mechanical coupling between adjacent rings. Since the ceramic has very little strength under tension, the stress rod and nut provide a stress bias to keep the ceramic under constant compression.

A number of possible causes of the current-runaway problem were investigated, with the final evidence pointing to the ceramic-stack resonators as the source of the problem. It was decided that experimental measurements of electrical input impedance vs frequency and temperature for the resonators in air might reveal the resonator problem.

With the method and equipment illustrated in Figure 2, individual resonators were driven in air in a temperature-controlled oven. The temperature of the air in the oven was changed in increments and allowed to stabilize for



30 min after each increment. At each temperature, the resonators were driven with a constant-amplitude, 10-V rms source that was swept in frequency over a range that included the operating band of the transducer. A typical result of electrical input impedance vs frequency and temperature is shown in Figure 3. The point of minimum impedance is the resonant frequency,  $f_m$ , and the point of maximum impedance is the antiresonant frequency,  $f_n$ . The overall electromechanical coupling in a resonator is generally proportional to  $\Delta f = f_n - f_m$ , while the overall resonator loss is inversely proportional to the spread between the impedance magnitudes at  $f_n$  and  $f_m$ ,  $\Delta Z = Z_n - Z_m$ . Note in Figure 3 the resonator's performance degradation with increasing temperature and the good recovery when the resonator was returned to room temperature (72°F). In a few of the resonators tested, the 250°F impedance magnitude vs frequency response was nearly flat, indicating severe degradation of the resonator performance. This behavior, shown for the impedance magnitude in Figure 4, occurred in only 3 of the 15 resonators tested. As a result of these initial tests it was concluded that increases in the ambient temperature of the individual resonators caused significant increases in dissipation and decreases in coupling which, in turn, (in a manner yet to be detailed) led to the current-runaway situation.



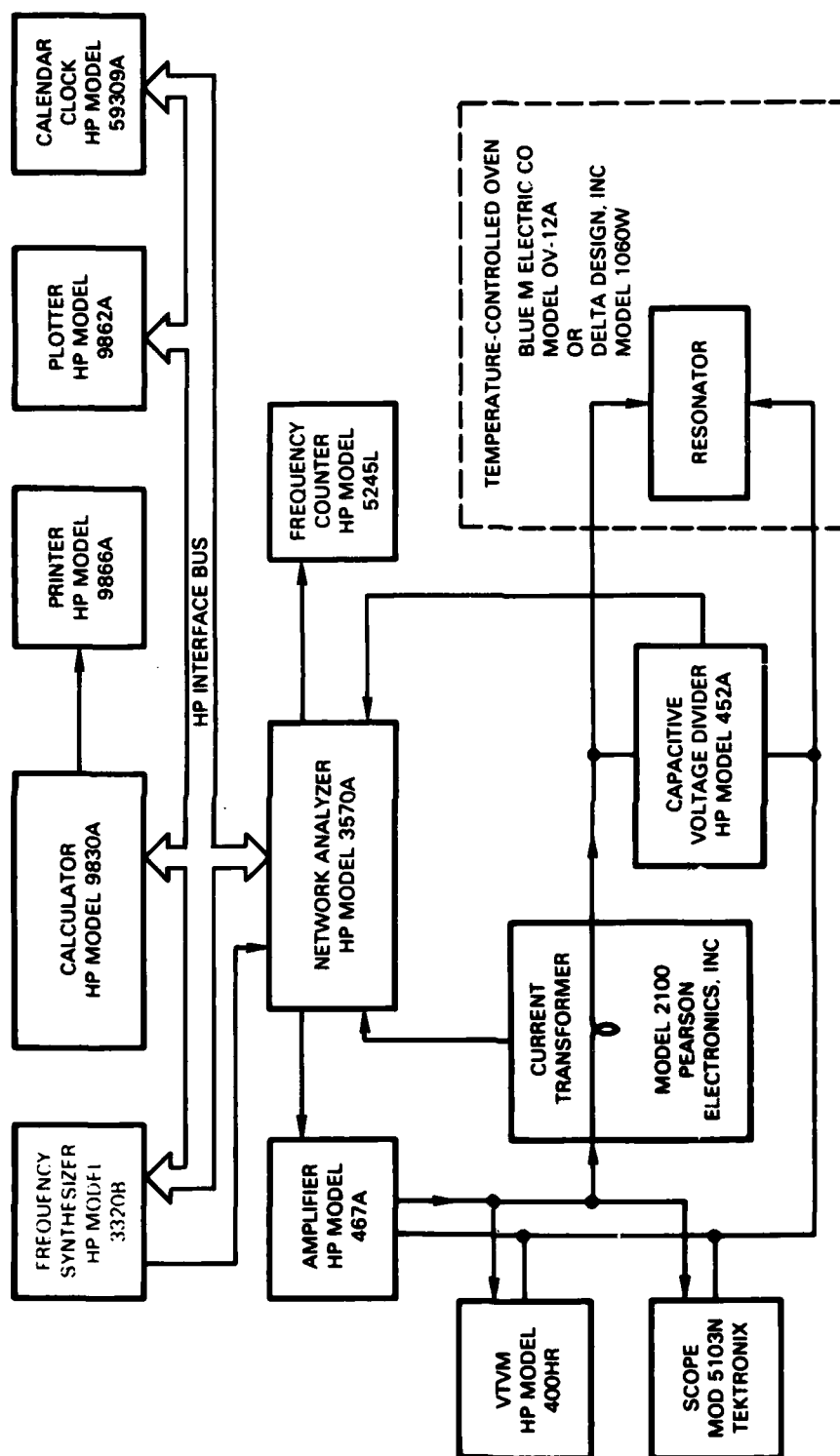


Figure 2. Block diagram of automated in-air impedance vs temperature measurements of longitudinal resonators.

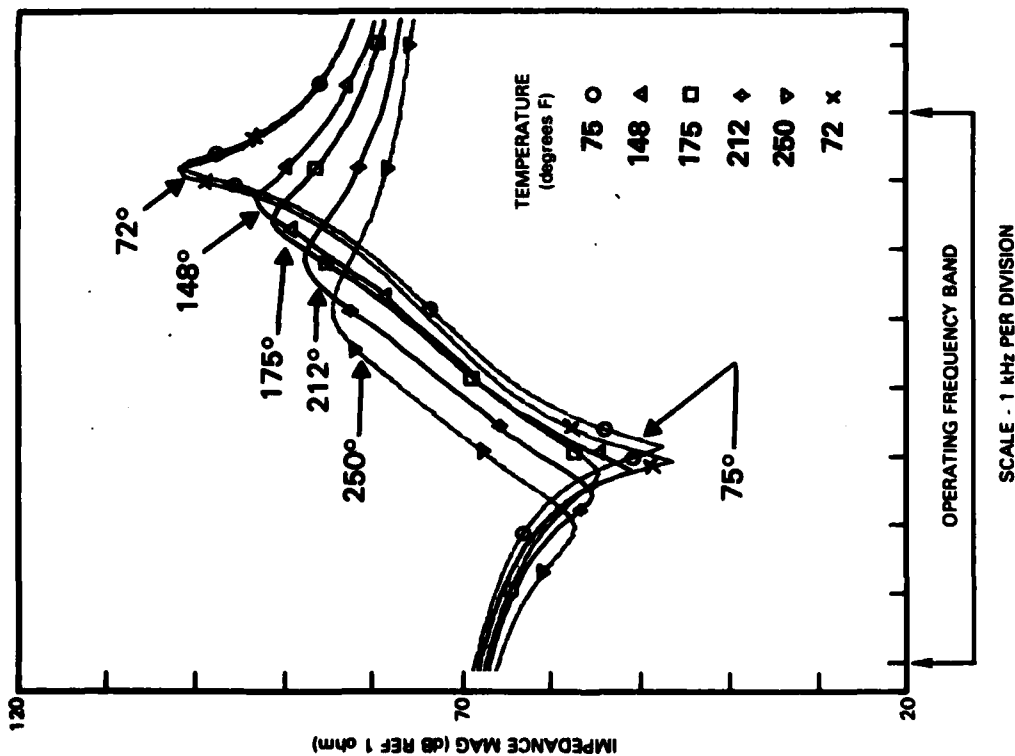


Figure 3. Impedance magnitude vs. frequency for "allegedly good resonator."

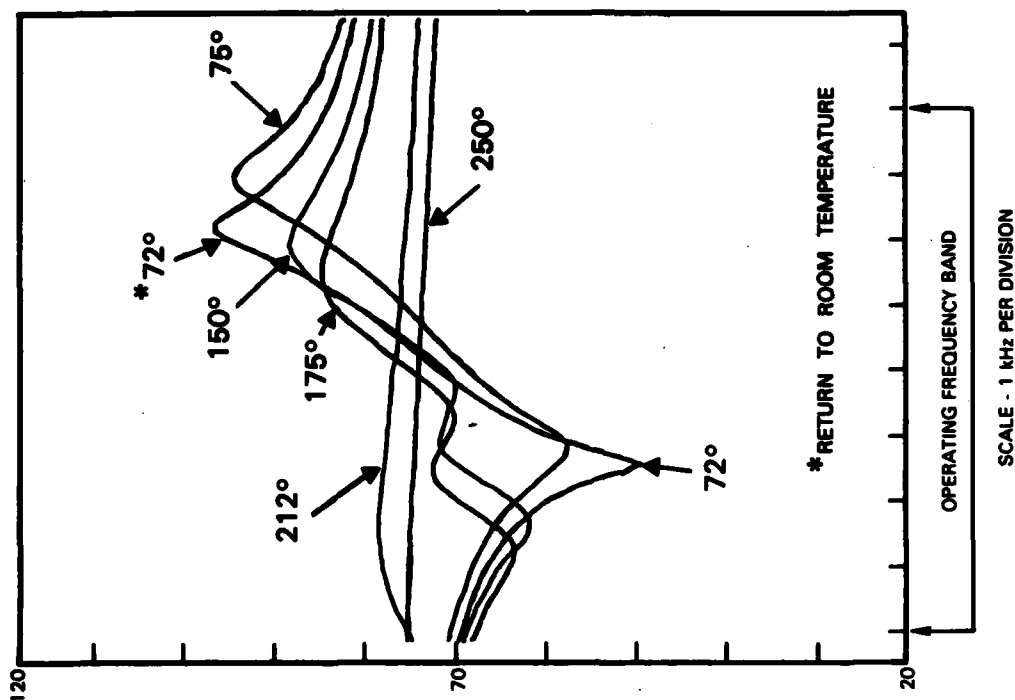


Figure 4. Impedance magnitude vs. frequency for "bad resonator."

## EXPERIMENTAL EVIDENCE OF CEMENT-JOINT PROBLEMS

Three possible explanations of the temperature-related resonator performance degradation were: the ceramic parameters might change significantly with temperature; the stress bias might be relieved at high temperatures due to unbalanced thermal expansion, resulting in ceramic-parameter changes; and the cement-joint\* properties might vary significantly with temperature. A ceramic manufacturer's published data (Reference 1) indicate that the ceramic frequency constant increases with temperature in the temperature range of interest. The frequency constant is the product of the resonant frequency and the ceramic length; thus the resonant frequency of the ceramic rings should increase with temperature, and the resonant frequency for the composite resonator should likewise increase. Since this is in opposition to the experimental results of decreasing resonant frequency with increasing temperature, the ceramic temperature behavior was ruled out as a cause of the resonator performance degradation with temperature.

In order to investigate the remaining two possibilities, a number of new resonators were built using differing construction methods. To investigate the possibility of stress bias relief, some resonators were built with a reduced-diameter stress rod, which results in more stretch of the rod for a given stress bias. In addition, some resonators were constructed with no cement, so that comparison of their experimental results with prior results for cemented resonators might indicate the role of cement-temperature effects. Figure 5 shows impedance magnitude vs frequency results for resonators containing different combinations of these two modifications.

Figure 5a presents results for a normal resonator modified to include a reduced-diameter stress rod. Since this modification increases the initial stretch of the stress rod, it should reduce any stress relief caused by

---

\*The joints in these types of resonators are referred to by many names, such as: ceramic-stack joints, cement joints, cement/electrode joints, adhesive joints, glue joints, and simply joints.

<sup>1</sup>"Piezoelectric Technology Data for Designers," Clevite Corp., Piezoelectric Division, 1965, Table III.

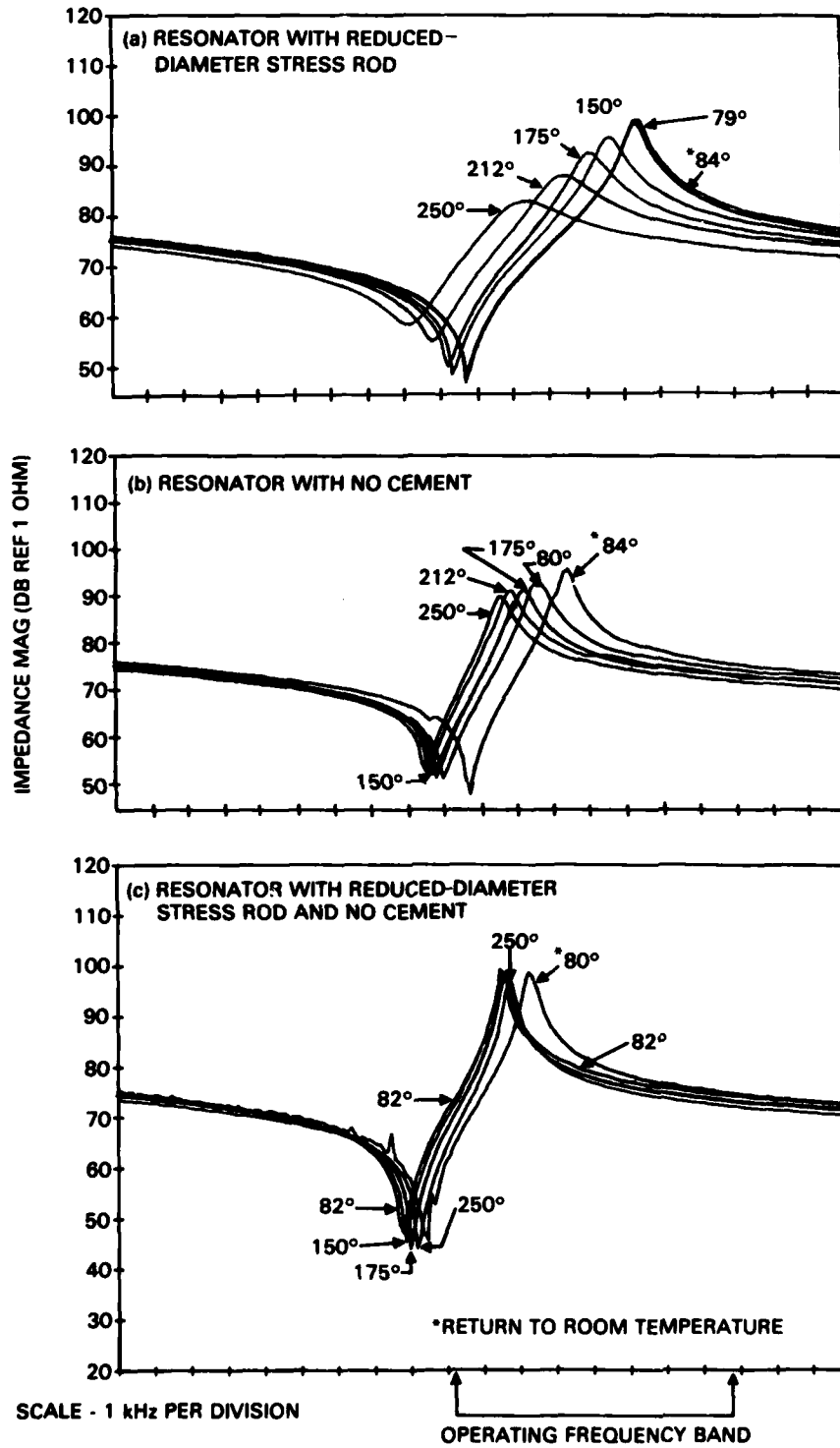


Figure 5. Experimental measurements for investigating cement and stress rod effects.

thermal expansion. Comparison of Figures 3 and 5a gives no clear indication that stress relief caused by thermal expansion plays an appreciable role in the temperature degradation of the resonators. Figure 5b shows results for a cementless resonator that is otherwise similar to the resonator of Figure 3. Both the frequency and magnitude at resonance and antiresonance are significantly less sensitive to temperature than is the case for the resonator in Figure 3. This indicates that the cement does play a substantial role in the temperature degradation. However, the fact that some temperature dependence remains and is generally removed by reducing the stress rod diameter, as seen in Figure 5c, suggests that stress bias relief due to thermal expansion is a minor contributor to the temperature dependence of the resonator. The fact that the reduction of the stress rod diameter had no apparent effect for a resonator containing cement (Figure 5a) indicates that the cement effects dominate and thus tend to mask any stress relief effects. In Figures 5b and 5c the results before and after the heat cycle do not agree. It is possible that the positioning of the resonator components had changed by the time the final room temperature (84°F and 80°F) measurements were taken (due to slippage in one or more of the cementless joints). However, this does not significantly alter the conclusions drawn above, especially those concerning the decrease of  $\Delta Z$  with increasing temperature.

Examination of the assembly procedures for the individual resonators revealed that a low torque was applied to the tail nut during curing of the cement. This procedure was estimated to result in only about 1000 psi of stress on the ceramic stack joints. Because this amount of stress was judged to be too low, a sample set of resonators was assembled with 4000 psi of stress. The increased stress caused the piezoelectric constant,  $d_{33}$ , to double for the assembled stack. Results for this high-stress resonator, as shown in Figure 6a, reveal a clear reduction in the temperature-related performance degradation. Although there was a definite decrease in resonator performance at temperatures above 212°F, the resonator was not expected to be subject to operating temperatures that high, so this was judged to be acceptable. In fact, later testing showed the new operating temperature of the stove to be about 150°F. Now, the higher prestress should have two direct results: the stress rod should be stretched more, and more cement should be

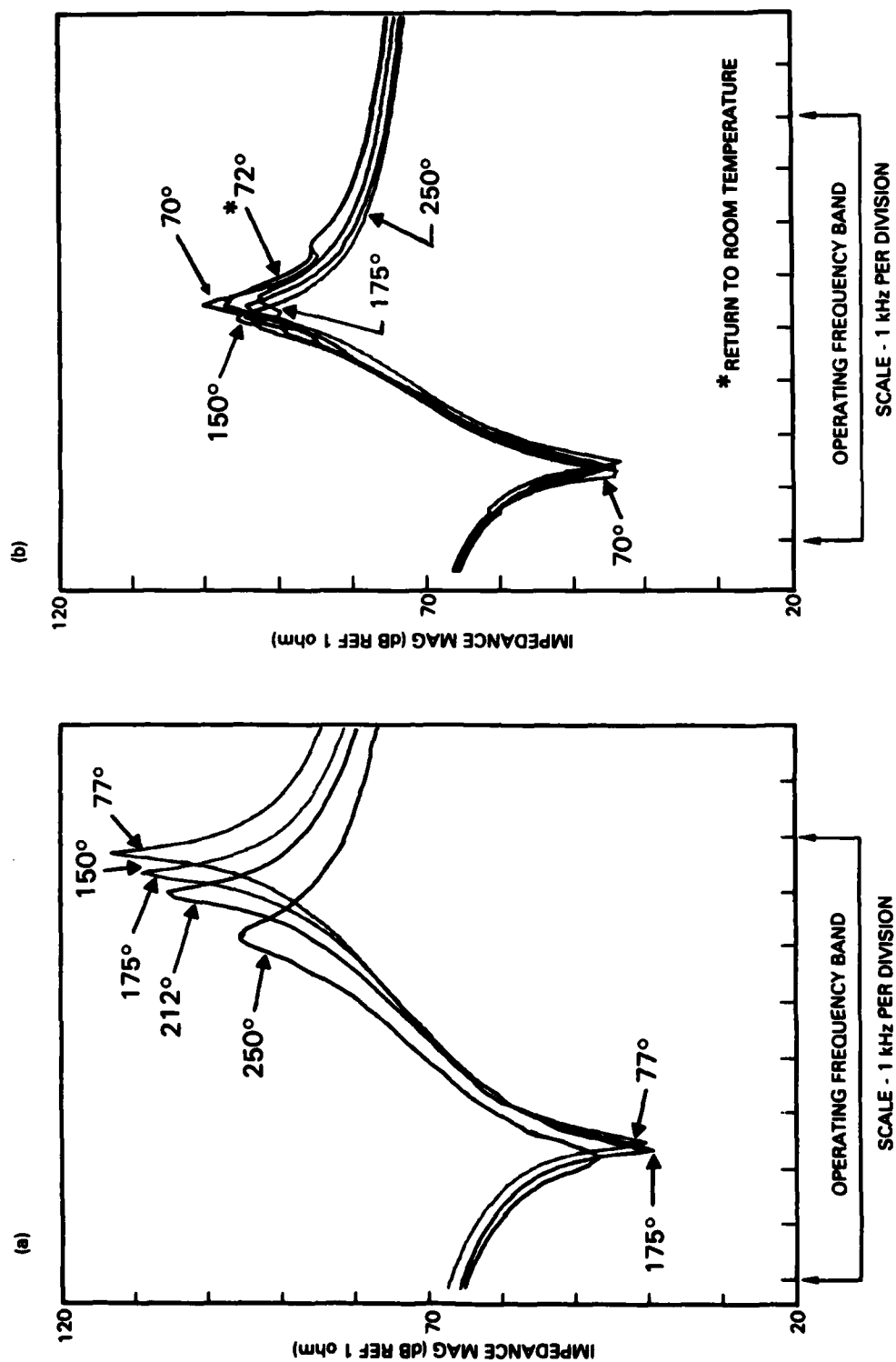


Figure 6. Experimental results for high-stress-bias resonators (a) with cement and (b) with no cement.

squeezed out of the joints, resulting in less cement in each joint. The latter is likely the main cause of the improved resonator performance. Results for a high-stress, cementless resonator, shown in Figure 6b, demonstrate that the remaining temperature effects in Figure 6a appear to be caused solely by the cement. The bumps in the curves in Figure 6b are probably the result of inconsistent coupling in the cementless joints. Note also that Figure 6a shows a marked increase in  $\Delta f$  and  $\Delta Z$  at all temperatures, indicating that at any temperature likely to be encountered in operation, this type of resonator should provide better performance than the lower stress resonators.

The experimental results in Figure 7 further support the hypothesis that the resonator performance degradation with temperature is related to the amount of cement in the joints. Measurements of impedance vs frequency and temperature are shown for three resonators that essentially differed from one another only in their cement/electrode joint configurations. Each resonator's joints differed from the others in two ways: the type of electrode, either solid or mesh (expanded metal), used in the joints; and the amount of stress bias applied during the curing of the cement. The final amount of cement in a joint should be less for higher stresses during curing, as stated, and also for the solid electrode as compared with the mesh electrode, since the mesh electrode will contain cement in the mesh holes. Therefore resonator 4812 should contain the most cement in its joints, resonator 735 less cement, and resonator 23 the least cement. The experimental results show that the temperature degradation of a resonator appears to increase with the amount of cement in the joints.

The experimental results in Figure 8 show correlation between the temperature dependencies of the cement tensile-shear strength and the resonator  $\Delta f$  values. All of the resonators used in the present study employed Epon VIII cement in the joints, and the cement joints were cured at 150°F for 2 to 3 hours. The available cement strength vs temperature data that came closest to meeting these cure conditions were for a 180°F 2-hour cure.\* The dashed

---

\* Shell Chemical Company data for Epon adhesives.

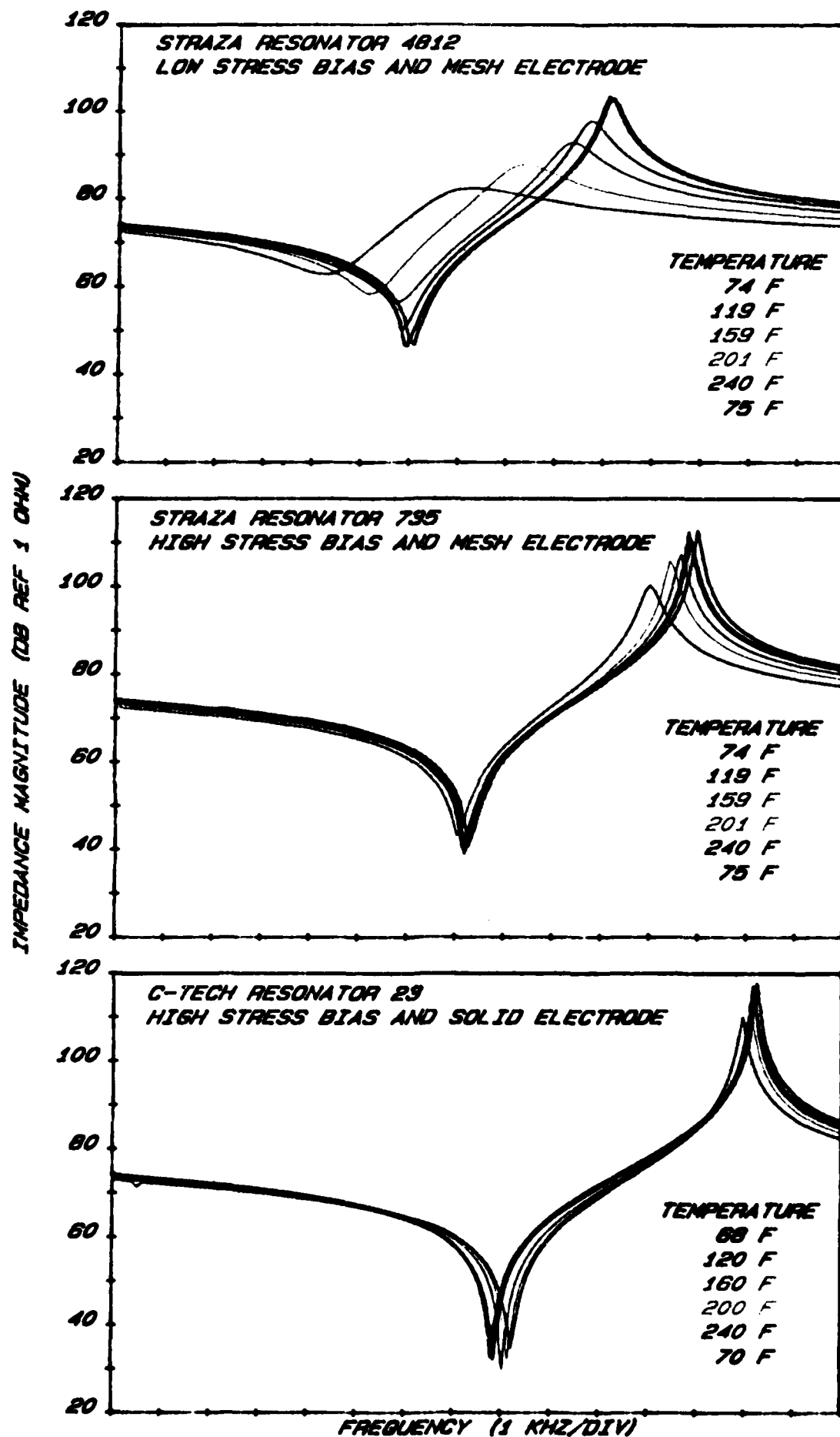
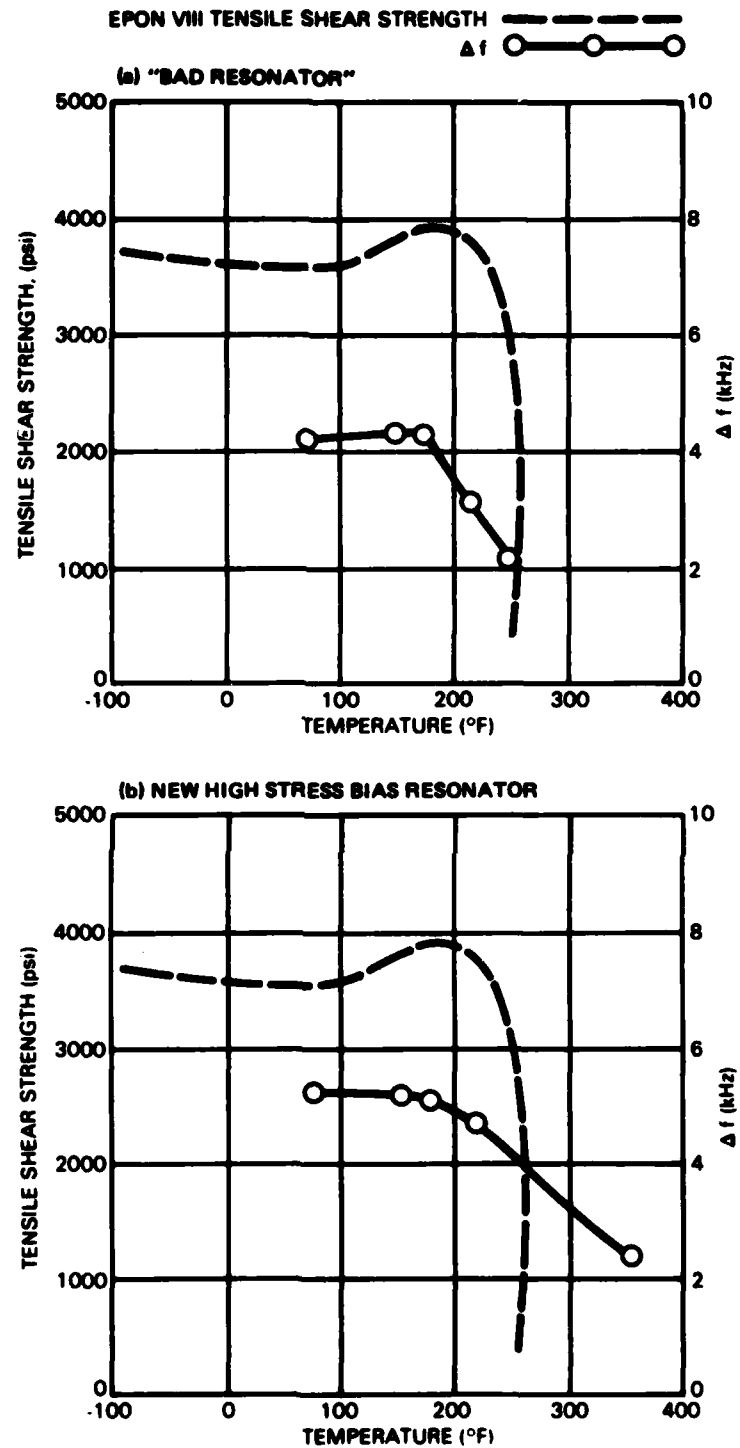


Figure 7. Experimental results for three resonators that differ in their cement/electrode joint configurations.





**Figure 8. Temperature dependence of  $\Delta f$  and cement strength.**

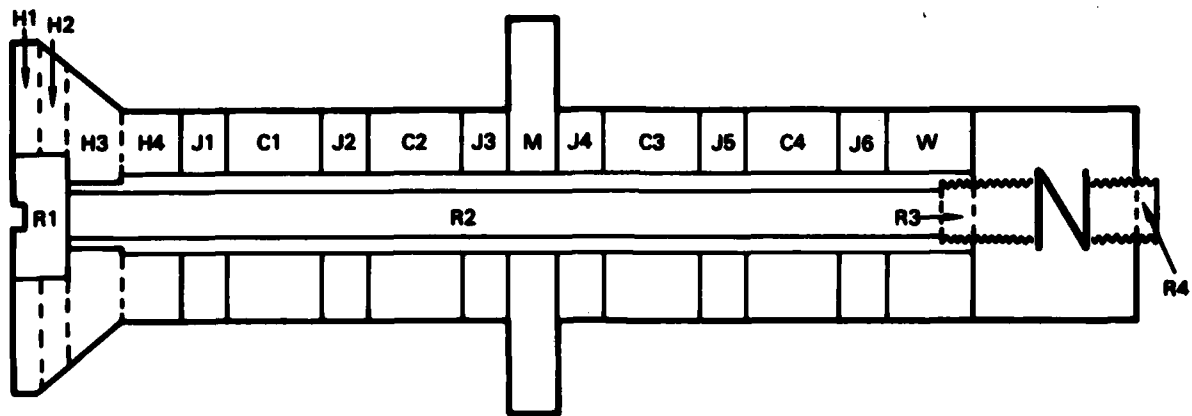
curves in Figure 8 represent this cement strength vs temperature data. The solid line in Figure 8a shows the frequency difference ( $\Delta f$ ) between resonance and antiresonance for the "bad resonator" (see Figure 4). The circles indicate the data points taken from the experimental results. Similarly, Figure 8b demonstrates the results for the new high-stress-bias resonator (see Figure 6a). Both of these results show correlation of the cement strength breakdown with the degradation in  $\Delta f$  as the temperature increases. Thus, these plots suggest that the increased compliance of the cement joints with temperature is a cause of the resonator performance degradation.

#### RESONATOR COMPUTER MODEL

A computer program has been developed to model a typical 33-mode piezoelectric ceramic stack resonator of the type shown in Figure 1. The resonator model is a plane wave model and has been developed using the SEADUCER computer program at the Naval Ocean Systems Center. The independent behavior of the expanded nickel electrodes in the joints is not clear. Therefore, in each joint the cement and electrode are combined as a single cement/electrode joint for modeling purposes.

Figure 9 shows a cutaway representation of the modeled resonator. The figure is not scaled, and the size of the joints has been greatly enlarged. Three basic types of sections are used in the model: straight nonceramic, conical nonceramic, and straight ceramic. The three types of sections are displayed in Figure 10 along with an equivalent circuit and the associated equations and parameters for each type of section. Each section of the resonator model has been labeled in Figure 9 for subsequent reference. H2 and H3 are conical nonceramic sections, C1 through C4 are straight ceramic sections, and the remaining sections are all straight nonceramic. The tail nut and the part of the stress rod that it covers have been combined in a single section (N).

An equivalent circuit representing the entire resonator as modeled by SEADUCER is presented in Figure 11. The Z's represent mechanical impedances, and the  $\gamma$  represents radiation impedance, with the superscripts denoting the different sections as labeled in Figure 9. In normal operation  $\gamma$  represents



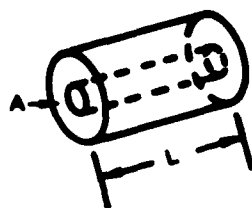
CERAMIC RINGS:	C1, C2, C3, C4
HEAD SECTIONS:	H1, H2, H3, H4
STRESS ROD SECTIONS:	R1, R2, R3, R4
TAIL NUT:	N
NODAL RING MOUNT:	M
CEMENT/ELECTRODE JOINTS:	J1, J2, J3, J4, J5, J6

Figure 9. Cutaway diagram of the resonator model.

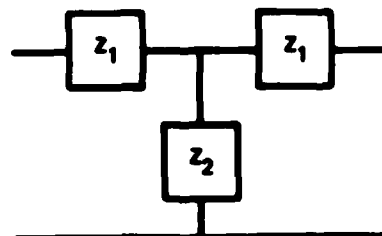
the radiation loading that the resonator encounters while mounted in the transducer. For resonator operation in air,  $\beta$  would be zero or represent a short in the circuit diagram. Electrical and mechanical losses are included in the ceramic sections by allowing  $g_{33}$ ,  $\epsilon_{33}^T$ , and  $s_{33}^D$  to be complex. Similarly, mechanical losses are included in the cement/electrode joints by allowing the sound velocity,  $c$ , to be complex. As can be seen by the equations in Figure 10, these complex parameters introduce a real part into the otherwise purely reactive impedances and, hence, result in power losses. The SEADUCER program uses a generalized multiport interconnection technique to set up matrix equations for the modeled resonator.

<sup>2</sup> H. H. Ding, L. E. McCleary, and J. A. Ward, Computerized Sonar Transducer Analysis and Design Based on Multiport Network Interconnection Techniques, NUC TP 228, April 1973.

(a) Straight nonceramic section

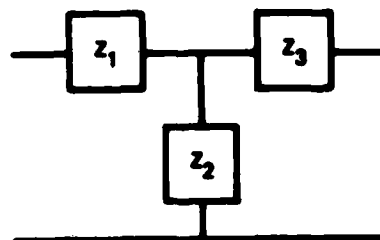
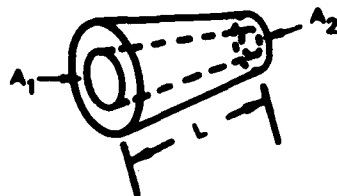


$$Z_1 = j\rho c A \tan kL/2$$



$$Z_2 = -j\rho c A \csc kL$$

(b) Conical nonceramic section



$$Z_1 = j\rho c \frac{\sqrt{A_1 A_2} - A_1 \cos kL}{\sin kL} - \frac{\sqrt{A_1 A_2} - A_1}{kL}$$

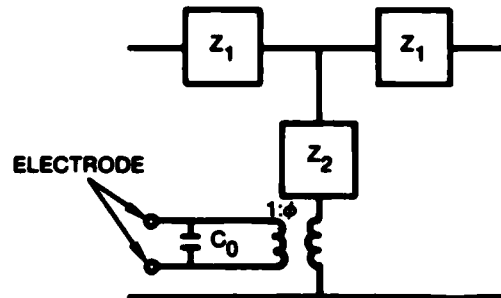
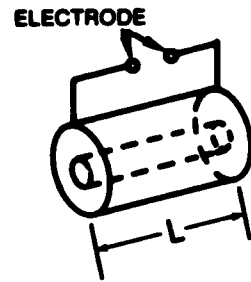
$$Z_2 = -j\rho c \sqrt{A_1 A_2} \csc kL$$

$$Z_3 = j\rho c \frac{\sqrt{A_1 A_2} - A_2 \cos kL}{\sin kL} - \frac{\sqrt{A_1 A_2} - A_2}{kL}$$

- L     = Length of section
- A     = Area of end surface
- $\rho$     = Density of material
- c     = Sound velocity in material
- $k = \omega/c$  = Wave number in material
- $\omega$     = Angular frequency

Figure 10. Types of sections used in the resonator model and their equivalent circuits.

(c) Straight ceramic section



$$Z_1 = j\rho c A \tan kL/2$$

$$Z_2 = -j(\rho c A \csc kL + \phi^2/\omega C_0)$$

$$C_0 = A/L\beta_{33}^{LC}$$

$$L = \text{length of ceramic section}$$

$$A = \text{area of end surface}$$

$$\rho = \text{density of ceramic}$$

$$k = \omega/c = \text{wave number in ceramic}$$

$$\omega = \text{angular frequency}$$

$$c = \text{sound velocity in ceramic}$$

$$\beta_{33}^{LC} = g_{33}^2/s_{33}^D + 1/\epsilon_{33}^T = 1/\epsilon_{33}^{LC} = \text{longitudinally clamped impermeability constant}$$

$$\phi = g_{33}C_0/s_{33}^D$$

$$g_{33} = \text{piezoelectric constant}$$

$$s_{33}^D = \text{elastic compliance at constant charge density}$$

$$\epsilon_{33}^T = \text{free dielectric constant}$$

Figure 10. (Continued.)

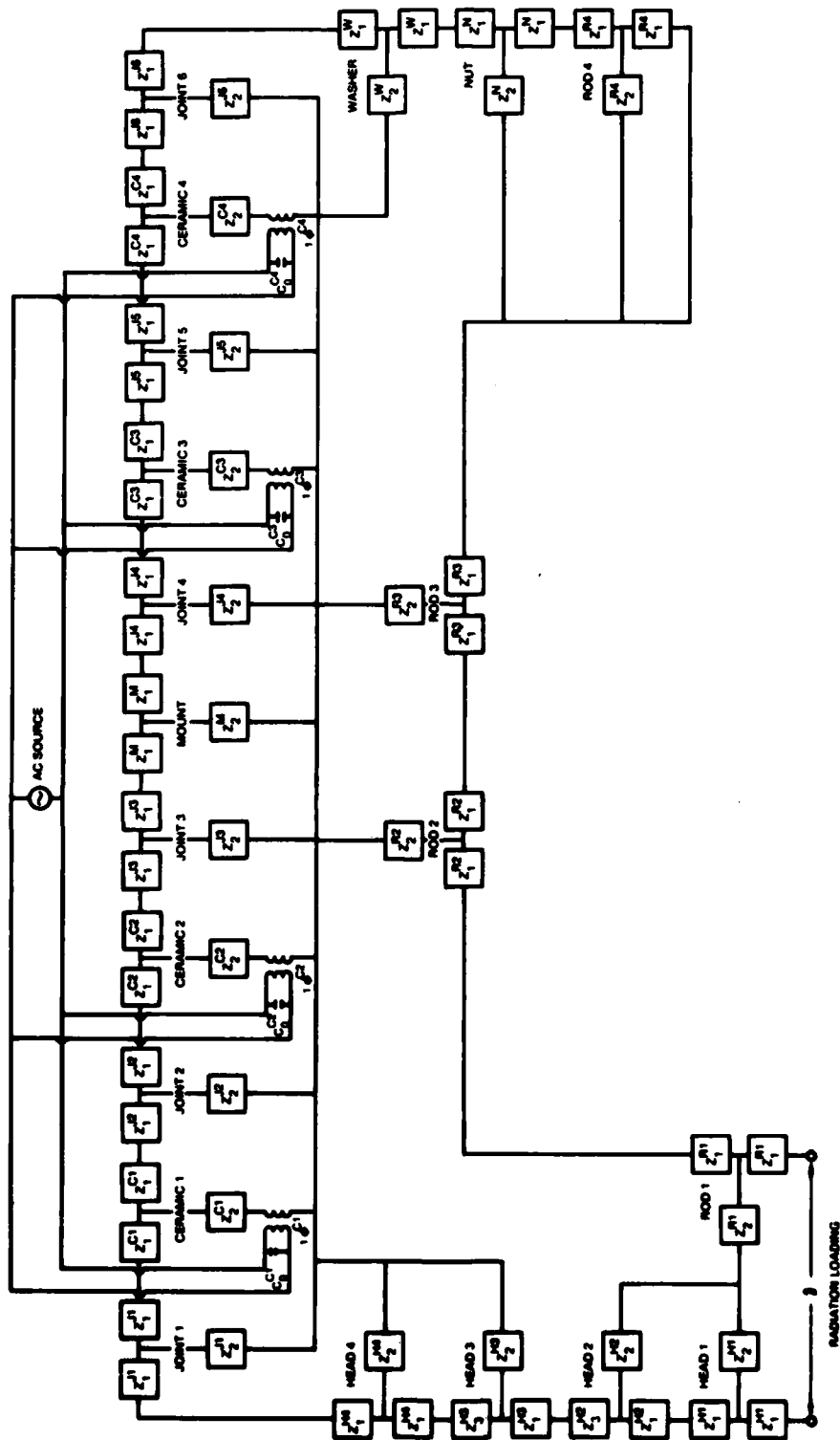


Figure 11. Equivalent circuit for model of ceramic stack longitudinal resonator.

The equations are then solved by standard matrix methods. Further details of the SEADUCER approach can be found in Reference 2.

A primary feature of the model is the capability to calculate the complex electrical input impedance as a function of source frequency. Another useful feature is the capability to estimate ceramic and joint parameters when first given certain experimentally obtainable data from a resonator. Many other types of results can easily be obtained by making minor modifications to the model. For example, calculation of power losses in the individual resonator components is a feature that should be implemented in the near future.

### MODELING RESULTS

Before discussing the modeling results it is useful to first explain the form that was used in this study for the complex ceramic and cement-joint parameters. Using  $p$  to represent any one of the complex parameters, we have used the form

$$p = p_r (1 \pm jp_m) \quad ; \quad p_m = \left| \frac{p_i}{p_r} \right|$$

where  $j$  is  $\sqrt{-1}$ , and  $p_r$  and  $p_i$  are, respectively, the real and imaginary parts of  $p$ . Losses are introduced by  $p_m$ , which is called the dissipation factor, loss tangent, or loss multiplier. The proper sign in the above equation is selected to assure power losses and not gains.

The computer model was exercised in a parameter-variation study for a resonator in air (no radiation loading). The study consisted of examining the impedance vs frequency results while independently varying the real part and dissipation factor of each of the ceramic and cement-joint parameters. The ceramic parameters of all four ceramic sections were varied together, as were the cement-joint complex sound velocities of all six joints. The ceramic parameters that were varied were the relative dielectric constant ( $\epsilon_{33}^T/\epsilon_0$ , where  $\epsilon_0$  is the free-space dielectric constant), the piezoelectric constant ( $g_{33}$ ), and the compliance ( $s_{33}^D$ ). Results from the parameter-variation study

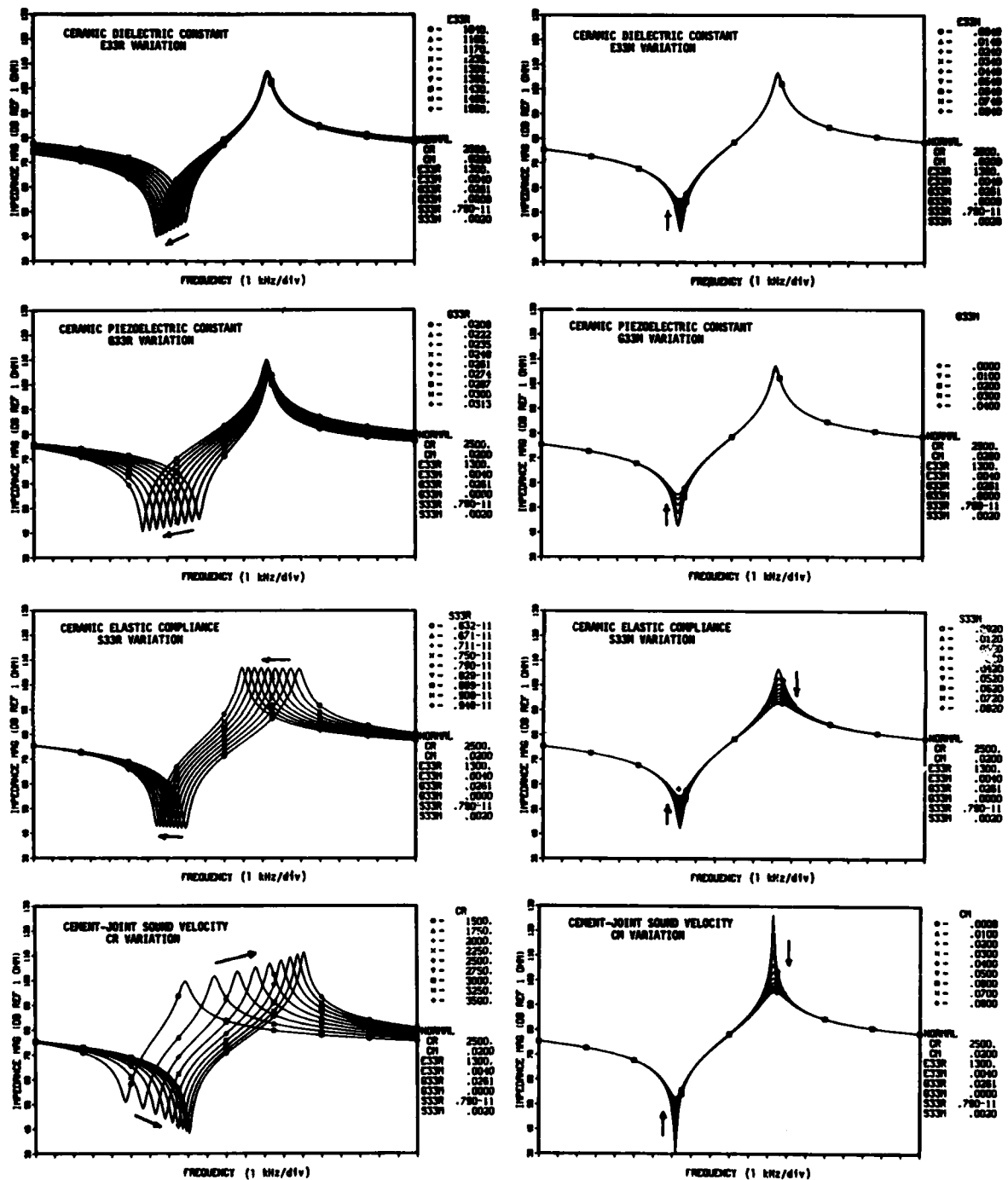


Figure 12. Parameter-variation study on a computer model of a 33-mode piezoelectric ceramic stack resonator.



are shown in Figure 12, in which R means the real part of the parameter, and M means the associated multiplier or dissipation factor (this notation was chosen for computer use). For example, for the piezoelectric constant, G33R is the real part of  $g_{33}$  and G33M is the  $g_{33}$  dissipation factor. It should be noted that E33R and E33M are for the relative dielectric constant  $\epsilon_{33}^T/\epsilon_0$ . In each plot, the item being varied is specified at the top, and the values it assumes are listed to the right of the plot (all units are MKS). For example, in the bottom left plot, the real part of c, the joint complex sound velocity, is varied from 1500 to 3500 m/s. In each plot all items other than the one being varied are set to "normal" values. The ceramic "normal" values were taken from a ceramic manufacturer's published data for type I (PZT4) ceramic (Reference 1). The cement-joint "normal" parameters were estimated from past experimental measurements. All of the parameter variations result in monotonic changes in the key features of the impedance vs frequency curves. Thus, arrows have been used to show the direction of the changes in these features as the parameter being varied increases in value.

Two observations that are apparent from examination of Figure 12 are: dissipation factors essentially affect only the impedance magnitudes at resonance and antiresonance and not the resonant and antiresonant frequencies themselves (Reference 3); the frequency and magnitude at antiresonance are almost entirely dependent on the two purely mechanical parameters  $s_{33}^D$  and c (in both their real parts and dissipation factors). Also, it is interesting to note that the combined variations of the cement-joint real sound velocity and associated dissipation factor would yield results very similar to the experimental results shown in Figures 3 and 4. This would apply if the joint sound velocity, CR, decreases with temperature and the dissipation factor, CM, increases with temperature.

Another application of the resonator model has been to estimate the cement-joint parameters for the three resonators of Figure 7, which contained different cement/electrode joint configurations. Experimental measurements of

<sup>3</sup>G. E. Martin, "Dielectric, Elastic and Piezoelectric Losses in Piezoelectric Materials," Ultrasonics Symposium Proceedings, IEE Cat #74 CH0896-ISU, 1974, p 613.

impedance vs frequency at room temperature are shown for each of the resonators by the solid curves in Figure 13. The dashed lines represent results from calculations using the resonator model. These three model results were selected from a limited joint-parameter variation study where only nine separate combinations of joint sound velocity and loss factor were examined. The ceramic parameters were kept constant at published room temperature values. Because of the limited number of cases (nine) to choose from, the model results represent only an initial attempt to match the experimental measurements. Although the matches are not the best that could be obtained, they are sufficient to permit estimation of the magnitude of the joint parameters for the three resonators. The joint sound velocity was the parameter that was varied in the modeling study; however, the joint stiffness is the more appropriate parameter of interest in this case. For example, for the two resonators that differ only in the amount of prestress applied during cement curing, it is not likely that the joint sound velocity differs, but rather that the joint stiffness does as a result of the final joint thickness. Because the joint thickness in the resonator is small ( $kL = 2 \pi L/\lambda \ll 1$ ), the  $Z_2$  impedance in the cement-joint equivalent circuit (Figure 10a) can be reduced to

$$Z_2 = jK/\omega$$

where  $K$  is the joint stiffness, given by

$$K = \frac{\rho c^2 A}{L}$$

with both  $K$  and  $c$  complex. Accordingly, a stiffness change can be represented in the model by a proper sound velocity change. Thus the labels for the model results in Figure 13 present this equivalent joint stiffness rather than the joint sound velocity.

The joints of the three resonators differ chiefly in the amount of cement they contain. Therefore, the estimated joint parameters from Figure 13 indicate that resonator 4812 contains the most cement, resonator 735 less cement, and resonator 23 the least cement, because the joint stiffness should decrease

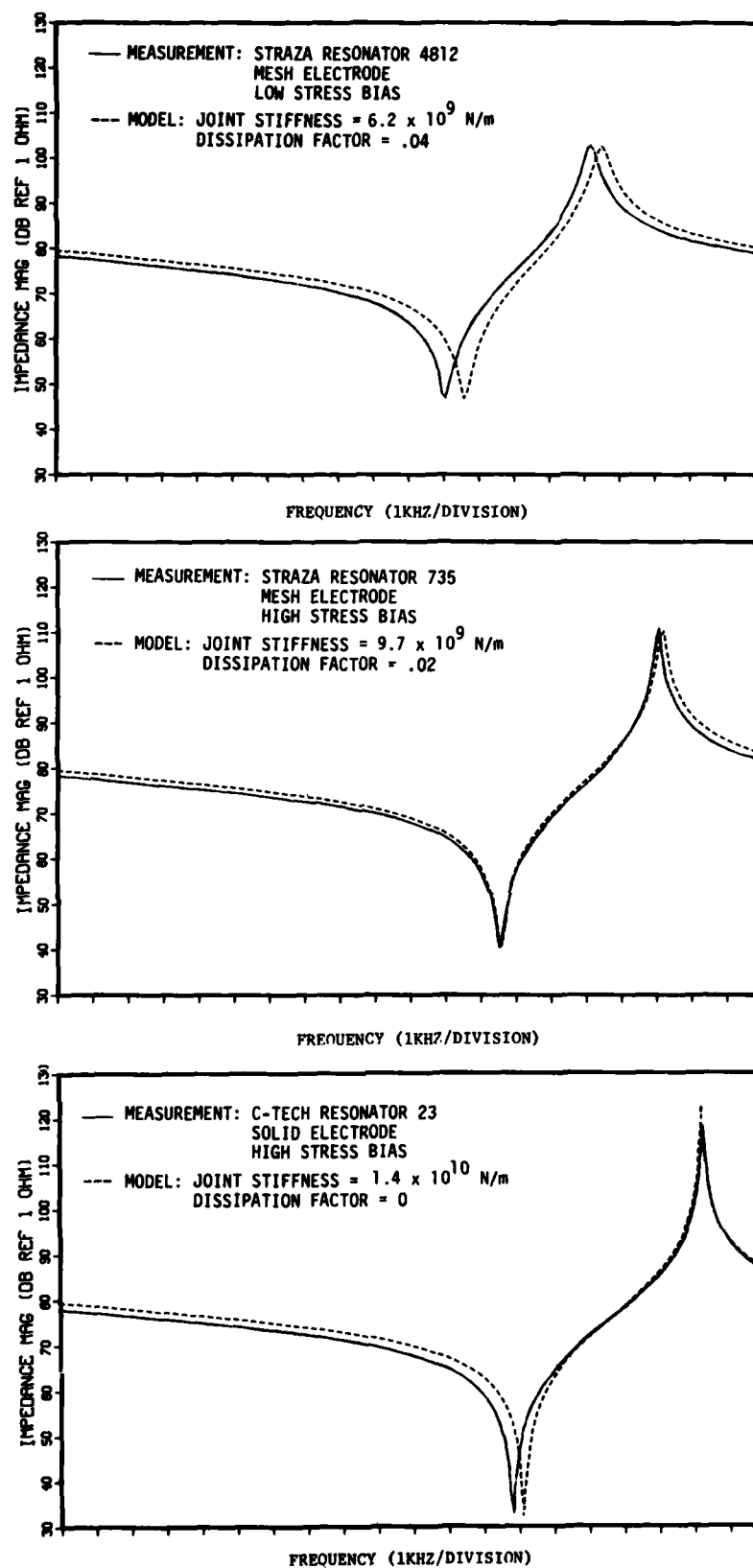


Figure 13. Estimation of joint parameters for three separate resonators by matching model results with experimental measurements.

as the amount of cement in the joint increases. This is in agreement with statements made above (p 12) based on the construction methods of the three resonators. Note also, that the estimated joint stiffness dissipation factor increases as the resonator performance degrades. It is not clear that the joint dissipation factor should differ for the three types of joints.

## CONCLUSIONS

The temperature-related performance degradation in ceramic stack resonators, associated with the current-runaway problem observed during the CUALT testing of certain transducers, has been investigated in this study by experimental and preliminary modeling efforts. The modeling is considered preliminary because the modeling must include ceramic and joint parameters as a function of temperature in order to draw final and detailed conclusions about the temperature-dependent resonator performance. The experimental and modeling results point to the cement joints of the resonators as the source of the problem. Present indications are that increasing cement compliance with temperature (and perhaps increasing dissipation factor) causes the resonator performance degradation. The improved temperature-related resonator performance that results from increased stress bias on the resonator during cement curing appears to be due to reduced amounts of cement in the resonator joints.

## RECOMMENDATIONS

Although the cement joint has been singled out as a prime contributor to temperature-related performance degradation in stacked ceramic resonators, significant work remains to be done to clearly explain the role that it plays. This work involves:

1. Obtaining ceramic and/or cement-joint parameter vs temperature data.
2. Applying the proper temperature-dependent ceramic and cement-joint parameters to in-air and radiation-loaded resonator models (perhaps guided by surface temperature measurements of in-air and dummy-loaded resonators) in order to obtain resonator performance as a function of temperature.
3. Exercising the "temperature-dependent" model in order to draw conclusions about the temperature-related role of cement joints in ceramic stack resonators and to determine general methods to eliminate or limit the cement joint effect.

## REFERENCES

1. "Piezoelectric Technology Data for Designers," Clevite Corp., Piezoelectric Division, 1965, Table III
2. H. H. Ding, L. E. McCleary, and J. A. Ward, Computerized Sonar Transducer Analysis and Design Based on Multiport Network Interconnection Techniques, NUC TP 228, April 1973
3. G. E. Martin, "Dielectric, Elastic and Piezoelectric Losses in Piezoelectric Materials," Ultrasonics Symposium Proceedings, IEE Cat #74 CH0896-ISU, 1974, p 613